Published in *Nuc. Instr. Methods Phys. A* **677**, 1-3 (2012).

A dynamically-adjustable wavelength-sensitive neutron filter

N. D. Vasilev[a], T. R. Charlton[b], O. Kirichek[b], C. J. Kinane[b], E. M. Schooneveld[b], S. Langridge[b], W. A. Kockelmann[b], P. V. E. McClintock[a],

[a] *Department of Physics, Lancaster University, Lancaster LA1 4YB, United Kingdom*
[b] *ISIS, STFC Rutherford Appleton Laboratory, Harwell Science and Innovation Campus, Didcot, OX11 0QX, United Kingdom*

Abstract

The prototype of a wavelength-sensitive neutron filter has been realized and tested successfully for the first time. The filter exploits the neutron wavelength dependence of the transparency of ^{3}He gas. The analysis of test results gives high wavelength resolution $\Delta\lambda/\lambda \simeq 0.5\%$ over the broad wavelength range 0.2 – 5.2Å. We propose an idea to expand the filter range in the short wavelength direction by use of a cryogenic environment, and also consider the use of media using other than ^{3}He gas. The proposed filter might be used in advanced reflectometers and SANS2D neutron scattering instruments.

Keywords: neutron filter, wavelength-sensitive neutron filter

1. Introduction

Gas detectors filled with ^{3}He are commonly used for the detection of thermal neutrons, due to their high efficiency and low gamma sensitivity [1]. Standard ^{3}He detectors on advanced neutron scattering instruments allow us to cover a broad range of scattering angles and momentum transfer vectors Q. For neutron spectroscopy, however, the need to measure the neutron energy transfers can make the instrument design much more complicated. In this paper, we describe a design and present test results for a wavelength-sensitive neutron filter. It has a wavelength resolution $\Delta\lambda/\lambda \simeq 0.5\%$ over the wavelength range $0.2 - 5.2\,$Å. We have also measured the neutron transparency of ^{3}He gas over the wide range of gas densities $7 \times 10^{-4} - 8 \times 10^{-3}\,\mathrm{g/\,cm^{-3}}$ in a cryogenic environment. The experimental data agree well with a simple model describing neutron transmission through the ^{3}He gas. They allow us

to extrapolate in order to estimate the range of applicability of the proposed filter at higher energies.

Measurements have been performed both at ambient temperature, by varying the gas pressure, and at cryogenic temperatures.

2. The filter principle

The filter consists of two time-of-flight monitors M1 and M2 and a thin-walled aluminium vessel of ^{3}He gas positioned between them. A neutron beam from a pulsed source passes through the first monitor M1, after that through the ^{3}He vessel and finally through the second monitor M2. The monitors measure the neutron counts as a function of time-of-flight. The variable ^{3}He pressure is used to decode the wavelength information of neutrons passing through the filter. By sweeping the ^{3}He pressure in the vessel, and then exploiting the fact that longer-wavelength neutrons are absorbed more than short-wavelength ones, we can build up a map of wavelength at the position of the detector. At high pressures nearly all long-wavelength neutrons are removed from the incident beam. Once having calibrated the filter in this way the system can be used as neutron energy analyzer. It is important to note that this energy analysis is performed in addition to the analysis of the wavelengths of neutrons in the incident beam via the time-of-flight techniques. Thus energy transfers can be measured with the proposed filter system. This principle should work for any absorber, not just ^{3}He.

3. Room temperature transmission measurements

We have carried out the first neutron transmission experiments on the filter at ISIS (Rutherford Appleton Laboratory). We used the ROTAX beamline [2] which currently serves as a sample characterisation, single-crystal alignment, and testing facility. ISIS is a pulsed source, so that the neutron wavelengths can be determined by measurement of their flight times. ROTAX views a cold (110 K) liquid CH_4 moderator; the flight path from the moderator to the sample position is 14.0 m. A 50 Hz background disk chopper is installed to remove gamma radiation and fast neutrons. For the present experiment the background chopper was de-phased, however, to gain access to the short-wavelength neutrons. The beam cross-section at the sample position was reduced to $10\times10\,\mathrm{mm}^2$ for the measurements. Two monitors measure the neutron counts as a function of time-of-flight. The cylindrical

^{3}He vessel between them had walls of 0.5 mm aluminium, with an outer diameter of 50 mm and length 55 mm. It was connected via a stainless steel capillary to a ^{3}He gas handling system that allowed the ^{3}He gas pressure to be changed from vacuum up to 10 bar.

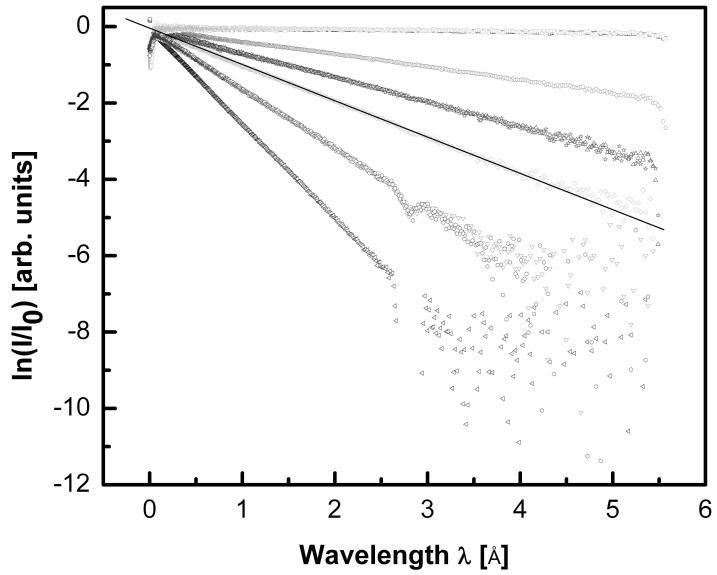

Figure 1: Transmission at various pressures for a ^{3}He filled can. The plots, from top to bottom respectively, correspond to the empty can and pressures of 1, 2, 3, 5 and 8 bar. One of the linear fits to the data is shown.

The repetition rate of the ISIS source is 50 Hz. The available time window for non-overlapping ISIS pulses on ROTAX is 0.7- 20 ms, corresponding to a wavelength band from 0.2 to 5.2 Å. The energy-resolution of the instrument is limited by the pulse-width of the moderator, which is about 35 μs at 2 Å (flux maximum), corresponding to a wavelength resolution $\Delta\lambda/\lambda \simeq 0.5\%$. Counts were accumulated in histograms as a function of time-of-flight using the standard ISIS data acquisition system. The front and rear monitors spectrums were corrected for efficiencies.In Fig. 1 the count-ratio between the front and rear monitors is plotted as a function of wavelength, measured for different pressures of the ^{3}He gas. The empty-cell count-ratio measurements

have been subtracted from the experimental data; Fig. 1 also includes the empty-cell data. The wavelength range with linear transmission through the ^{3}He is from 0.2 to 2.5 Å. The linear section of the plot for a given pressure can be used to determine the neutron wavelength. Its slope depends only on the ^{3}He density, as will be shown below. The count rates deviate from the linear transmission behaviour due to dead-time effects of the monitors at short wavelength, and due to the background chopper at about 2.8 Å. At longer neutron wavelengths, where practically all neutrons are absorbed in the ^{3}He gas, the instrumental background (scattered neutrons and gamma quanta) and detector noise start to dominate. These regions of data can safely be ignored.

4. Cryogenic temperature transparency measurements

In order to achieve good resolution in the upper part of the energy range one needs a higher density of ^{3}He gas. This can be achieved either by increasing of the gas pressure in the vessel, or by cooling the ^{3}He gas to liquid helium temperatures. The high pressure case has several disadvantages such as requirements for thick vessel walls and a special high pressure gas handling system for loading ^{3}He into the vessel. Give the cost of the gas, and the small quantities available, the practical realization of such a system is non-trivial. To investigate the opportunity of using the cryogenic option, we therefore performed neutron ^{3}He transparency measurements at low temperature.

The fluid ^{3}He sample was contained in a cylindrical aluminum cell of internal diameter 31.4 mm, length 67.0 mm and wall-thickness 0.5 mm. It was maintained in the temperature range 1.25 - 50 K in the variable temperature insert of a Variox cryostat. The temperature of the cell was measured by a Cernox temperature sensor. The high purity ^{3}He gas was supplied to the cell through a stainless steel capillary of internal diameter of 1.1 mm. The establishment of thermal equilibrium was confirmed by means of a pressure gauge. A schematic diagram of the CRISP neutron reflectometer, configured for low temperature experiments, can be found in [3]. The instrument passes the pulsed neutron beam from ISIS via a 20 K hydrogen moderator to provide neutron wavelengths in the range 0.5 – 6.5 Å. The CRISP instrument was set up in transmission geometry with the neutron beam passing through the vapor above the liquid ^{3}He surface. Below the ^{3}He critical temperature T_c the liquid-vapor interface was found by scanning the height of the sample cell with the neutron beam. The resultant neutron intensity versus height plot

took the form of a step function, with no measurable intensity when the beam was incident only on the liquid filled portion of the cell. All transmission measurements were taken with the neutron beam well above of the liquid surface.

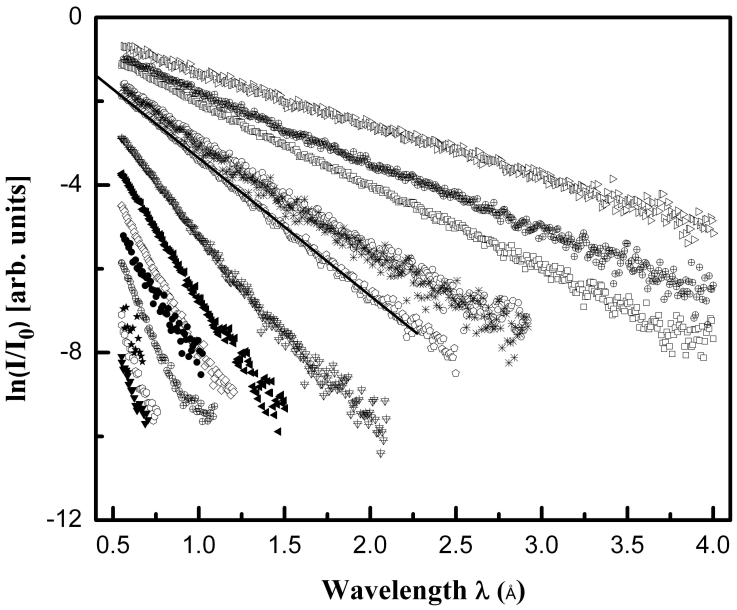

Figure 2: Linear dependence of intensity as a function of wavelength for 14 different temperatures and one example of linear fit. The temperatures corresponded to the plots, from top to bottom respectively, were 50.0, 1.4, 1.46 1.53, 20.0, 1.75, 2.0, 10.3, 2.35, 7.0, 2.55, 3.0, 2.73, and 4.35 K.

We measured the incident and transmitted neutron intensities through ^{3}He vapor as a function of temperature. The intensities obtained were then corrected for detector efficiency before calculation of the transmittance. The transmission through the evacuated, empty cell was also checked. However taking into account that the neutron absorption of the filled cell is much higher at low temperatures due to the higher density of 3He gas we have considered that the vessel corrections were unnecessary.The logarithm of normalized intensity as a function of wavelength for a range ^{3}He vapor temperatures is plotted in Fig. 2. It is evident that the experimental data can be

very well-fitted by straight lines. The transmission of neutrons through ^{3}He gas is governed by

$$\ln(I/I_0) = (-nl\sigma_0/\lambda_0)\lambda \quad (1)$$

where n is the ^{3}He concentration, $l = 29.12\,\mathrm{mm}$ is the average distance the beam travels through the cell, which depends on the cell radius and the beam width, $\sigma_0 = 6049.3\,\mathrm{barn}$ is the absorption cross-section at a given wavelength λ_0=2.0334 Å (reference), and λ is the neutron wavelength. In this formula $\sigma_0\lambda/\lambda_0$ represents the wavelength-dependent cross-section [4]. We know that $\tau = (-nl\sigma_0/\lambda_0)$ is the slope of the data in Fig. 1 and Fig. 2. We also know that it varies as a function of pressure. There are two ways make use of this on a neutron instrument:

We treat the cell as a filter with a variable wavelength response. Here we would vary the pressure from transparent to opaque while making many neutron measurements in between. This filter would be placed between the sample and the detector. We would then need to use Equation (1) (but rearranged) to calculate the wavelength of the neutron as we vary the pressure in the cell.

From Equation (1) we can obtain the average density: $n = -\lambda_0\tau/l\sigma_0$ in units of atoms/cm^3, which we determined by linear least-squares fitting (Fig. 2 and Fig. 1). We can rewrite this in units of $\mathrm{g\,cm^{-3}}$ as $\rho = -\lambda_0\tau A/l\sigma_0 N_A$, where A is the ^{3}He atomic weight, and N_A is Avogadro number. Using this approach we can obtain the density of ^{3}He vapor from our experimental neutron transmission data. These results, together with those obtained by refractive index and permittivity measurements [5, 6] are presented in Fig. 3. It is clearly evident that, far from the critical temperature T_c, both methods yield similar results. However, near the critical temperature of $T_c \sim 3\,\mathrm{K}$, the densities obtained from neutron transmission results are lower than those published in [5, 6]. This is the region where neutron opalescence effects are expected to become significant. In particular, during opalescence any microscopic thermal fluctuations become strongly correlated leading to large-scale density fluctuations. Good agreement of density data at high temperatures implies that neutron transparency does not depend on temperature other than trivially due to the density change. This allows us to suggest that our model can be used in entire temperature range from 1K up to ambient temperature.

In principal the analysis shown here is valid for any neutron absorber. Although expensive, ^{3}He still has the advantage of an easy-to-control density when compared with other popular neutron absorbers such as Boron based

gases, Cd, Gd, or Borated ceramic. However, ^{3}He is becoming scarcer and more expensive on account of the global ^{3}He supply shortage [7]. Boron-based gases, e.g. BF_3, provide a viable alternative in terms of density control, but are typically difficult to handle due to their corrosiveness and/or explosive nature.

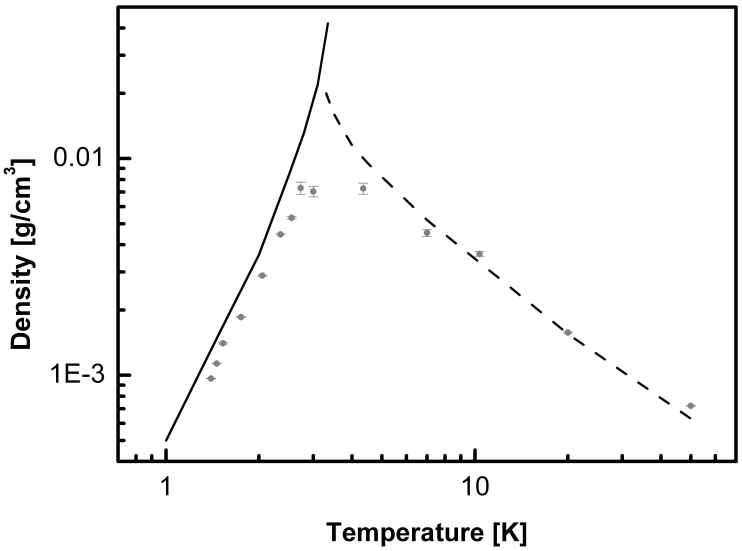

Figure 3: The ^{3}He fluid density as a function of temperature. Our experimental data (circles) are compared with earlier density data [5] (dashed line measured for ^{3}He gas at 1 bar pressure) and [6] (full line measured at the ^{3}He saturated vapor pressure) over a broad temperature range. The error estimates originate from the standard deviation of the slopes extracted from linear fits to the data shown in (Fig. 2).

The adjustable wavelength-sensitive filter described in this paper can be used in temperature range 5 - 300K with advantage as a neutron energy analyzer in neutron reflectometry and SANS instruments, especially where a broad energy range of incident neutrons is required. The application range of the proposed detector may be extended to neutron energies corresponding to production through nuclear fission reactions, or for non-proliferation treaty verification, or for security applications.

We thank the ISIS sample environment group for valuable technical assistance. The work was supported by STFC and EPSRC (Ref. N EP/F021429/1).

[1] E. M. A. Hussein, Handbook on Radiation Probing, Gauging, Imaging and Analysis, Kluwer, Dordrecht (2003).

[2] W. Kockelmann, M. Weisser, H. Heinen, A. Kirfel, W. Schafer, in R. Delhez, E. Mittemeijer, eds., European Powder Diffraction, Pts. 1&2 in series Material Science Forum, vol. 321–3, Trans Tech, Stafa-Zurich, 332–337.

[3] T. R. Charlton, R. M. Dalgliesh, O. Kirichek, S. Langridge, A. Ganshin, P. V. E. McClintock, Low Temp. Phys. 34 (2008) (4-5) 316.

[4] J. Als-Nielsen, O. Dietrich, Phys. Rev. 133 (1964) (4B) B925.

[5] V. P. Peshkov, Sov. Phys. JETP 18 (1948) (10) 857.

[6] E. R. Grilly, E. F. Hammel, S. G. Sydoriak, Phys. Rev. 75 (1949) (7) 1103.

[7] A. Cho, Science 326 (2009) (5954) 778.